Article

Quercetin Regulates the Polarization of Microglia through the NRF2/HO1 Pathway and Mitigates Alzheimer's Disease

Ying Feng[1,†]
Xinjun Yu[1,*,†]
Jingyang Han[1]

[1]Geriatric Medicine Department, Affiliated Hospital of Shandong Second Medical University, 261041 Weifang, Shandong, China

Abstract

Background: Alzheimer's disease (AD) is a burdening disease and is the main cause of dementia. Quercetin (Que), an antioxidant, plays potential roles in treating age-related disorders, including AD. This study aimed to validate the effects of Que on AD and explore the underlying mechanisms.

Methods: Mice with no treatment, amyloid-β Aβ (1-42) treatment (for acquiring AD model), or Aβ (1-42) plus Que treatment were used. Cognitive function was determined using the open field test (OFT), objective recognition test, and Y-maze test. In brain tissues, mRNA levels of inflammation cytokines, the M1 microglia marker cluster of differentiation (CD)86, and the M2 microglia markers arginase 1 (Arg1) and CD206 were measured. Nuclear factor E2-related factor 2 (NRF2)/heme oxygenase-1 (HO1) pathway-related proteins were detected by western blot. Additionally, mechanisms were investigated using human microglia HMC3 cells treated with Aβ (1-42) and Aβ (1-42) plus Que. The NRF2/HO1 pathway in HMC3 cells was inhibited using the selective inhibitor ML385. Cell viability and death were assessed using the cell counting kit-8 (CCK-8) and lactate dehydrogenase (LDH) release levels, respectively. Cell apoptosis was measured by terminal deoxynucleotidyl transferase-mediated dUTP nick-end labeling (TUNEL). Levels of NRF2/HO1 pathway-related proteins, inflammation cytokines, and oxidative stress-related markers, including malondialdehyde (MDA), superoxide dismutase (SOD), and glutathione (reduced glutathione (GSH)/oxidized glutathione disulfide (GSSG)), were determined in HMC3 cells. Flow cytometry was used to determine M1 markers CD86 and CD80 and M2 markers CD206 and CD163.

Results: Cognitive ability was impaired in AD model mice, and Que treatment reversed this impairment ($p < 0.05$). Levels of interleukin (IL)-1β, tumor necrosis factor-alpha (TNF-α), and IL-6 were increased, while M2 markers were decreased in the AD model mouse brain. Que treatment reversed these changes ($p < 0.001$). The NRF2/HO1 pathway was slightly inhibited in AD mice brain, while further activated by Que ($p < 0.05$). Que reversed the Aβ (1-42)-impaired cell viability. Through greatly activating NRF2/HO1 pathway, Que suppressed Aβ (1-42)-induced cell death, decreased Aβ (1-42)-promoted IL-1β, TNF-α, IL-6, MDA, CD86 and CD80, increased Aβ (1-42)-suppressed SOD and GSH/GSSG, and greatly increased CD206 and CD163 ($p < 0.01$).

Conclusion: Quercetin, through the activation of the NRF2/HO1 pathway, promotes M2 polarization of microglia, suppresses Aβ (1-42)-induced inflammation and oxidative stress, protects microglia from Aβ (1-42)-induced damage, improves cognitive function in mice, and demonstrates therapeutic potential for AD.

Keywords

Alzheimer's disease; quercetin; microglia; NRF2/HO1; polarization

Introduction

Alzheimer's disease (AD) is characterized by amyloid-β plaques and neurofibrillary tangles, presenting primarily as a progressive amnestic disorder that evolves into an amnestic-predominant, multidomain dementia.

*Corresponding author details: Xinjun Yu, Geriatric Medicine Department, Affiliated Hospital of Shandong Second Medical University, 261041 Weifang, Shandong, China. Email: yuxinjun9779@163.com
†These authors contributed equally.

This condition is burdensome and lethal [1,2]. Recent data indicate that the prevalence of dementia will double in Europe and triple worldwide by 2050, with AD being the leading cause of dementia [3,4]. Consequently, more research into AD is warranted to develop effective therapies for treating AD and its associated dementia.

Quercetin (Que) is a unique subclass of flavonoid that facilitates various physiological and biochemical processes in plants by acting as an antioxidant [5]. Que has demonstrated its antioxidant properties *in vivo* and *in vitro* [6]. Its ability to scavenge free radicals makes it a potent molecule for treating age-related disorders and health-related issues [7,8]. Notably, Que has shown promising therapeutic potential for AD due to its neuroprotective properties, including protecting neurons from oxidative damage, inhibiting amyloid-β fibril formation, and regulating inflammation and cell lysis [9,10]. However, the relationship between Que and AD requires further verification, and the underlying mechanisms need more exploration and understanding.

Neuroinflammation is considered a leading cause of AD [11,12]. Microglia, the resident macrophages in the brain, play a role in amyloid-β accumulation. The M1 microglia phenotype is associated with neuronal damage and oxidative stress, whereas the M2 phenotype helps regulate neuroinflammation by clearing damaged cells and generating new neurons [13,14]. Antioxidant activity is related to the activation of nuclear factor E2-related factor 2 (NRF2) by increasing antioxidant proteins and achieving neuroprotection [15]. Decreased levels of NRF2 and its target gene, heme oxygenase-1 (HO1), have been observed in AD brains, and NRF2 is known to interfere with multiple processes during AD [15].

In this study, we further demonstrated that Que ameliorates AD through *in vivo* and *in vitro* experiments. We also explored the associations between the underlying mechanisms, microglial polarization, and the NRF2/HO1 pathway. The results of this study provide deeper insights into how Que treats AD, offering potential therapeutic strategies for AD treatments.

Materials and Methods

Preparation of Animals

A total of thirty male wild-type C57BL/6 mice (30 ± 3 g), aged 12–13 months, were obtained from The Jackson Laboratory (Bar Harbor, ME, USA). The mice were housed under controlled conditions with 50–60% humidity, a temperature of 21–23 °C, and a 12-hour light/dark cycle. Standard food and water were provided ad libitum. All animal studies were ethically approved by the Ethics Committee of Shandong Second Medical University (Approval No. 2024SDL065).

Animal Grouping and Treatments

The mice were randomly divided into 3 groups (10 mice/group): negative control (NC), AD, and AD + Que. NC group mice were maintained without further treatments. AD group mice were induced with amyloid-β (Aβ) (1-42)-induced AD. Briefly, mice were anesthetized with an intraperitoneal injection of 50 mg/kg pentobarbital sodium (P3761, Sigma-Aldrich, Bellefonte, PA, USA). Subsequently, 3 µL of Aβ (1-42) (HY-P5905, MedChemExpress, Monmouth Junction, NJ, USA) dissolved in DMSO at a concentration of 220 pmol/µL was administered via intracerebroventricular injection (i.c.v.) [16]. The injection coordinates relative to bregma were –0.1 mm anteroposterior, –1.8 mm dorsoventral, and –0.75 mm mediolateral [17]. The mice were then maintained in standard conditions.

AD + Que group mice were induced with Aβ (1-42) as described for the AD group and then treated with Que (60 mg/kg/day; HY-18085, MedChemExpress, Monmouth Junction, NJ, USA) via intraperitoneal injection for 49 days [18]. Following treatments, all mice underwent cognitive tests. Subsequently, the mice were euthanized with an intraperitoneal injection of 180 mg/kg pentobarbital sodium (P3761, Sigma-Aldrich, Bellefonte, PA, USA). Brain tissue samples were collected, frozen in liquid nitrogen, and stored at –80 °C.

Open Field Test (OFT)

The OFT was conducted to measure the locomotor activity of the mice. Each mouse was placed in the center of a plastic box (50 cm × 50 cm × 50 cm) and allowed to move freely for 5 minutes while being recorded by a camera (Z 7II, Nikon, Tokyo, Japan). The distance traveled by each mouse was analyzed using Smart 3.0 software (PanLab, Irvine, CA, USA) to represent the spontaneous activity.

Objective Recognition Test

The object recognition was performed using Smart 3.0 software, as previously described [19]. The time spent by a mouse with its nose within 2 cm of an object was recorded as the exploration time. Recognition capability was determined using the discrimination index (%): 100% × [(time

of new object exploration – time of familiar object exploration)/(time of new object exploration + time of familiar object exploration)].

Y-Maze Test

The Y-maze test was performed as previously described [20]. The alternation percentage (%) was calculated as: 100% × (alteration numbers)/(total arm entry numbers – 2). Additionally, the time spent in the novel arm (%) was calculated as: 100% × (time in the novel arms/total time in arms).

Real-Time Reverse Transcriptase-Polymerase Chain Reaction (RT-qPCR)

RNA was extracted from brain tissues using TRIzol® reagent (DP424, Tiangen, Beijing, China) following the manufacturer's instructions. RNA purity was assessed (OD 260 nm/OD 280 nm = 1.8–2.2) using a full-wavelength spectrophotometer (OSE-260, Tiangen, Beijing, China). The RNA was then reverse-transcribed into cDNA using the FastQuant cDNA synthesis kit (KR116, Tiangen, Beijing, China). RT-qPCR was performed using a fluorescence quantitative instrument (LightCycler96, Roche, Shanghai, China). Relative expression levels were normalized to *β-actin* using the $2^{-\Delta\Delta Cq}$ method for data analysis. Primer sequences are listed in Table 1.

Table 1. Primer sequences.

Name	Sequence (5′-3′)
Mice *IL-1β*	F: CCCATCCTCTGTGACTCATGG
	R: CATCTCGGAGCCTGTAGTGC
Mice *TNF-α*	F: ACCGCAACAACGCCATCTAT
	R: GTATCAGTGGGGGTCAGCAG
Mice *IL-6*	F: AGACAAAGCCAGAGTCCTTCA
	R: GGTCCTTAGCCACTCCTTCTG
Mice *CD86*	F: ACGATGGACCCCAGATGCACCA
	R: GCGTCTCCACGGAAACAGCA
Mice *Arg1*	F: CTTGCGAGACGTAGACCCTG
	R: TCCATCACCTTGCCAATCCC
Mice *CD206*	F: TCAGCTATTGGACGCGAGGCA
	R: TCCGGGTTGCAAGTTGCCGT
Mice *β-actin*	F: CTGTCCCTGTATGCCTCTG
	R: ATGTCACGCACGATTTCC
Human *IL-1β*	F: GGGATAACGAGGCTTATGTGC
	R: AGGTGGAGAGCTTTCAGTTCA
Human *TNF-α*	F: TGAGCACTGAAAGCATGATCC
	R: GGAGAAGAGGCTGAGGAACA
Human *IL-6*	F: GACCCAACCACAAATGCCAG
	R: GAGTTGTCATGTCCTGCAGC
Human *β-actin*	F: CTCTTCCAGCCTTCCTTCCT
	R: AGCACTGTGTTGGCGTACAG

IL, interleukin; *TNF-α*, tumor necrosis factor alpha; *Arg1*, arginase 1; *CD206*, cluster of differentiation 206; F, forward; R, reverse.

Western Blot

Nuclear and total proteins were extracted using a protein extraction kit (P0028, Beyotime, Shanghai, China) supplemented with phenylmethanesulfonyl fluoride (PMSF; ST507, Beyotime, Shanghai, China). Proteins were separated by sodium dodecyl sulfate-polyacrylamide gel electrophoresis (SDS-PAGE; 10%, P0012, Beyotime, Shanghai, China) and transferred onto nitrocellulose membranes (IPVH15150, Millipore Sigma, Billerica, MA, USA). Primary antibodies from Abcam (Cambridge, UK) were used, including anti-NRF2 (1:1000 dilution, ab62352), anti-HO1 (1:1000 dilution, ab13248), anti-Histone-3 (1:1000 dilution, 4499, Cell Signaling Technology (CST), Danvers, MA, USA), anti-cluster of differentiation (CD)86 (1:1000 dilution, ab239075), anti-arginase 1 (Arg1) (1:1000 dilution, ab215843), anti-CD206 (1:1000 dilution, ab64693), and anti-glyceraldehyde-3-phosphate dehydrogenase (GAPDH; 1:2000 dilution, ab8245). Membranes were incubated with secondary antibodies (1:2000 dilution, ab6721, ab6728, Abcam, Cambridge, UK) for 2 hours, and proteins were visualized using an enhanced chemiluminescent (ECL) substrate (P0018, Beyotime, Shanghai, China). Grey values were analyzed using Image J software (1.48, National Institutes of Health, Rockville, MD, USA).

Cell Culture and Treatments

Human microglial cells HMC3 (iCell-h301, iCell Biosciences Inc., Shanghai, China) were cultured in a specific medium (iCell-h301-001b, iCell Biosciences Inc., Shanghai, China) at 37 °C, 70%–80% humidity, and 5% CO_2. The short tandem repeat (STR) profiling authenticated the cell line, and mycoplasma testing confirmed no contamination. Que toxicity was assessed by cell viability after treatment with various Que concentrations for 24 hours. The effect of Que against Aβ (1-42) was evaluated by the cell viability after treatment with Que and Aβ (1-42) for 24 hours. Cells in the Control group were cultured without further treatment. Cells in the Aβ (1-42) group were treated with 1 μM Aβ (1-42) [13]. Cells in the Aβ (1-42) + Que group were treated with 1 μM Aβ (1-42) and 5 μM Que. For further NRF2 inhibition, the selective NRF2 inhibitor ML385 (5 μM; HY-100523, MedChemExpress, Monmouth Junction, NJ, USA) was used to treat cells in the Aβ (1-42) + Que + ML385 group.

Cell Viability

Cell viability was determined using the cell counting kit-8 (CCK-8) assay kit (C0037, Beyotime, Shanghai, China). Cells were seeded in 96-well plates (1×10^4 cells/100 µL) and cultured for 24 hours, followed by treatment for an additional 24 hours as designed. Subsequently, 5 µL of CCK-8 reagent was added to cells for a 1-hour incubation in the dark. Absorbance was measured at 570 nm using a microplate reader (CMax Plux, Molecular Devices, Shanghai, China).

Terminal Deoxynucleotidyl Transferase-Mediated dUTP Nick-End Labeling (TUNEL) Assay

Apoptosis was assessed using the TUNEL assay kit (C1088, Beyotime, Shanghai, China). Cells were washed with phosphate-buffered saline (PBS; C0221A, Beyotime, Shanghai, China) and stained with 4′,6-diamidino-2-phenylindole (DAPI; C1005, Beyotime, Shanghai, China). Stained cells were visualized under a fluorescence microscope (CKX53, Olympus, Tokyo, Japan) to quantify apoptotic cells. The mean count of TUNEL-positive cells was calculated from three selected microscopic fields.

Enzyme-Linked Immunosorbent Assay (ELISA)

Cell culture supernatants were collected, and various contents were measured using ELISA kits from Abcam (Cambridge, UK), including lactate dehydrogenase (LDH; ab183367), interleukin (IL)-1β (ab214025), IL-6 (ab178013), tumor necrosis factor-alpha (TNF-α; ab181421), malondialdehyde (MDA; ab287797), and from Beyotime (Shanghai, China) including superoxide dismutase (SOD; S0101S), glutathione (reduced glutathione (GSH) and oxidized glutathione disulfide (GSSG); S0053).

Flow Cytometry

Cell surface markers were stained with primary antibodies (Abcam, Cambridge, UK) at 4 °C for 30 minutes, including anti-CD86 (1:500 dilution; ab239075), anti-CD80 (1:400 dilution; ab225674), anti-CD206 (1:500 dilution; ab270634), and anti-CD163 (1:12,500 dilution; ab314947). Cells were treated with Goat Anti-Rabbit IgG H&L (ab150077, Abcam, Cambridge, UK) at 4 °C for 30 minutes. Cells were washed, resuspended in PBS, and analyzed using a flow cytometer (FC500 MLP, Beckman Coulter Inc., Brea, CA, USA).

Statistical Analysis

Data were expressed as means ± standard deviation (SD). Group comparisons were conducted using GraphPad Prism 8.0.2 (GraphPad Software Inc., San Diego, CA, USA), employing analysis of variance (ANOVA) and Tukey's test. Statistical significance was considered at $p < 0.05$.

Results

Que Mitigates Cognitive Impairment in AD Model Mice

No significant difference in total distance was observed (Fig. 1A). However, the results of the objective recognition test (Fig. 1B) demonstrated that the discrimination index significantly decreased in AD mice models ($p < 0.001$) and significantly increased following Que administration ($p < 0.001$), indicating that Que improved Aβ (1-42)-induced impairment of spatial and working memory in AD mice. The spontaneous alteration (Fig. 1C) was significantly decreased in AD mice ($p < 0.001$) but was significantly improved by Que treatment ($p < 0.01$), indicating that Que mitigated spatial memory deficits. Additionally, the time spent exploring the novel arm (Fig. 1D) significantly reduced in the AD group ($p < 0.001$) but significantly increased in the AD + Que group ($p < 0.01$), demonstrating that Que mitigated spatial recognition deficits. Collectively, these results indicate that Aβ (1-42) impaired the cognitive abilities of AD model mice, while Que ameliorated these impairments.

Que Attenuates Neuroinflammation, Promotes M2 Polarization, and Activates the NRF2/HO1 Pathway in AD Model Mice

Inflammatory cytokines (Fig. 2A–C) were significantly upregulated in brain tissues of AD mice ($p < 0.001$), while Que administration significantly reduced their expression levels ($p < 0.001$), demonstrating that Que decreased neuroinflammation in the brains of AD mice. The M1-specific marker CD86 (Fig. 2D) was increased in the brains of AD mice and was decreased by Que treatment, though the change was not statistically significant. Conversely, M2-specific markers of Arg1 (Fig. 2E) and CD206 (Fig. 2F) were significantly reduced in AD mice ($p < 0.001$) but significantly upregulated by Que treatment ($p < 0.001$). Western blot analysis showed no significant differences in CD86 protein expression among the NC, AD, and AD + Que groups (Fig. 2G,H). In contrast, Arg1 and CD206 protein expression levels were significantly reduced in AD

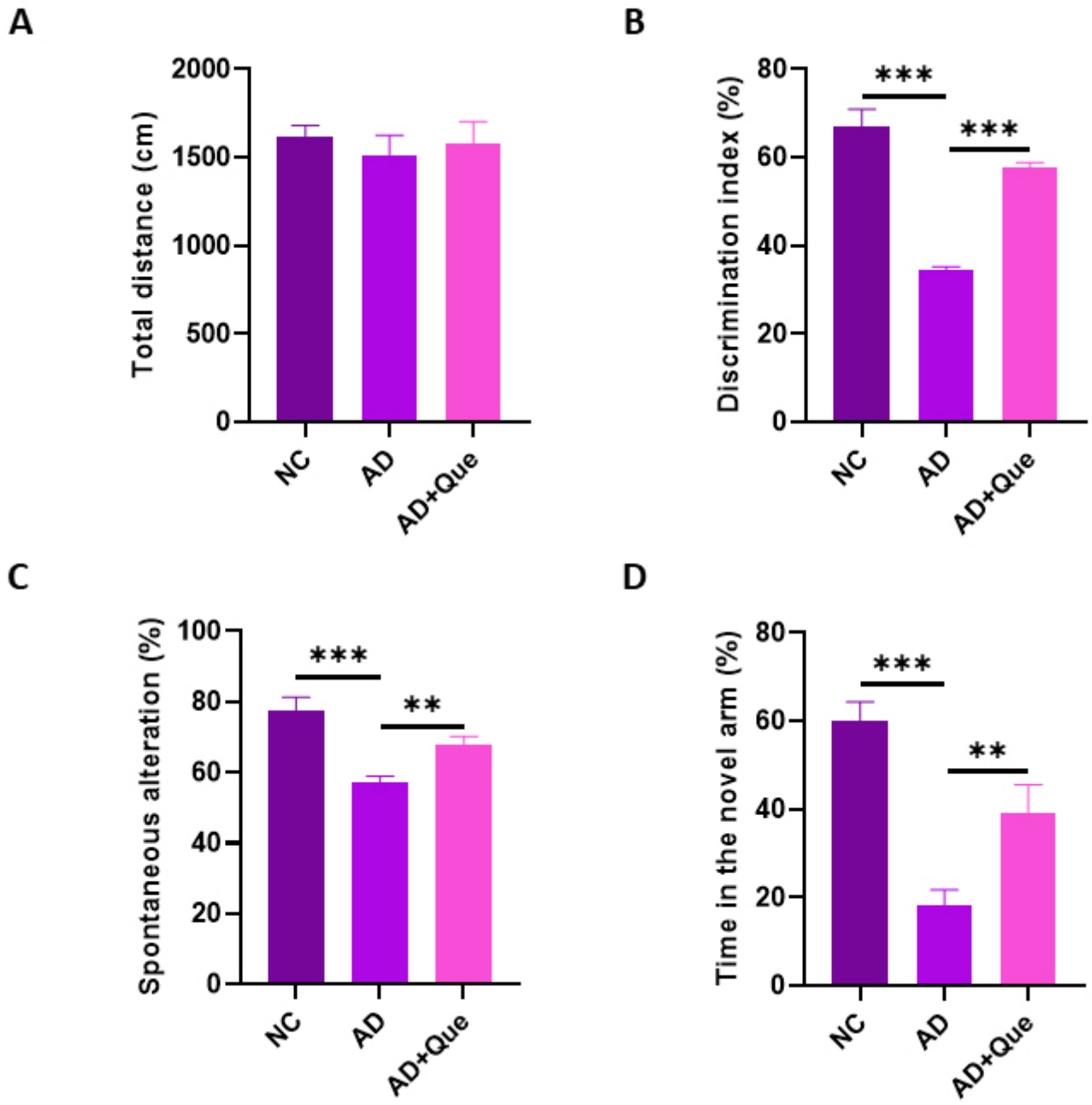

Fig. 1. Que mitigates cognitive impairment in Alzheimer's disease (AD) model mice. (A) Open field test (OFT) results showing the total distance traveled by mice (ANOVA). (B) Objective recognition test results (ANOVA). (C,D) Y-maze test results (ANOVA). n = 10. $^{**}p < 0.01$, $^{***}p < 0.001$. Abbreviations: NC, negative control (mice with no treatments); AD, Alzheimer's disease (mice injected with amyloid-β (Aβ (1-42); 222 µM, 2 µL) to induce AD); AD + Que, Alzheimer's disease mice treated with Aβ (1-42) (222 µM, 2 µL) and quercetin (Que; 60 mg/kg). ANOVA, analysis of variance.

group mice compared to the control group, but Que treatment markedly increased their levels ($p < 0.001$) (Fig. 2I,J). These findings indicated that M2 microglia polarization was suppressed in AD mice brains, while Que promoted M2 polarization. Furthermore, the results in Fig. 2K demonstrated that nuclear NRF2, total NRF2 and HO1 were significantly downregulated in AD mice brain tissues ($p < 0.05$), and Que treatment further significantly increased these levels ($p < 0.05$), indicating that the Que activated the NRF2/HO1 pathway.

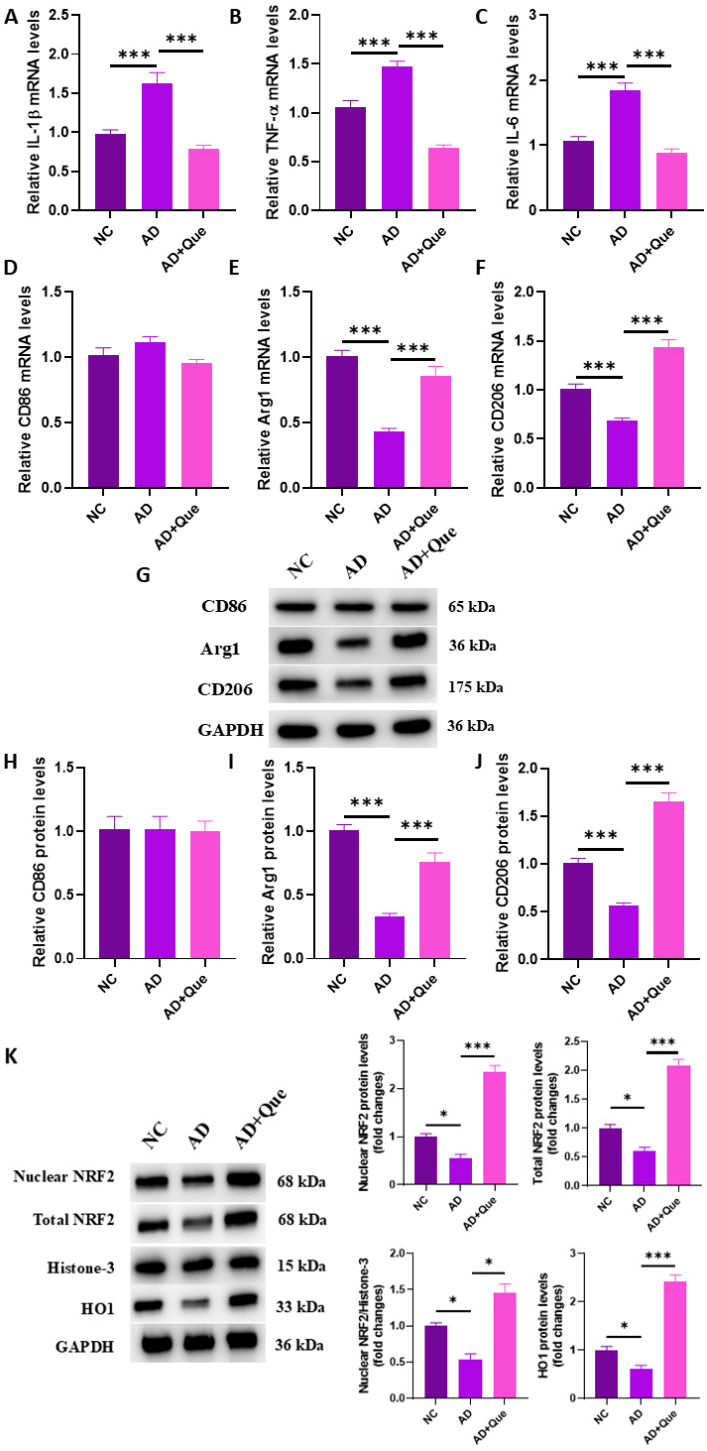

Fig. 2. Que attenuates neuroinflammation and promotes NRF2/HO1 pathway activation in AD model mice. (A–C) Levels of inflammatory cytokines interleukin (IL)-1β (A), tumor necrosis factor-alpha (TNF-α; B), and IL-6 (C) (ANOVA). (D) mRNA level of M1 microglia marker cluster of differentiation 86 (CD86) (ANOVA). (E,F) mRNA levels of M2 microglia markers arginase 1 (Arg1; E) and cluster of differentiation 206 (CD206; F) (ANOVA). (G–J) Protein levels of M1 microglia marker CD86 (H) and M2 microglia markers Arg1 (I) and CD206 (J) (ANOVA). (K) Levels of NRF2/HO1 pathway-related proteins (ANOVA). n = 10. *$p < 0.05$, ***$p <$ 0.001. Abbreviations: NC, negative control; AD, Alzheimer's disease; Que, quercetin; IL, interleukin; TNF-α, tumor necrosis factor alpha; Arg1, arginase 1; CD206, cluster of differentiation 206; NRF2, nuclear factor E2-related factor 2; Histone-3, Histone H3; HO1, heme oxygenase-1; GAPDH, glyceraldehyde-3-phosphate dehydrogenase.

Que Elevates Cell Viability and Activates the NRF2/HO1 Pathway in Microglial Cells

As shown in Fig. 3A, cell viability remained unchanged when microglial HMC3 cells were treated with various concentrations of Que. Fig. 3B shows that Aβ (1-42) significantly decreased HMC3 cell viability ($p < 0.001$), while Que treatment significantly increased cell viability ($p < 0.05$). These results suggest that Que reversed the impairment of microglial cell viability caused by Aβ (1-42), with 5 μM Que showing the most potent effect. Thus, 5 μM Que was used for subsequent experiments. As shown in Fig. 3C, the NRF2/HO1 pathway-related nuclear NRF2, total NRF2 and HO1, were significantly downregulated by Aβ (1-42) treatment ($p < 0.05$), and further increased by Que treatment ($p < 0.001$), indicating that Que promoted NRF2/HO1 pathway activation in Aβ (1-42)-treated microglial cells. Additionally, ML385 (a selective NRF2 inhibitor) treatment significantly decreased the levels of NRF2/HO1 pathway-related proteins ($p < 0.05$), indicating that ML385 inhibited the NRF2/HO1 pathway.

Que Decreases Cell Death of Aβ (1-42)-Treated Microglia by Activating the NRF2/HO1 Pathway

The release of LDH (Fig. 4A) in HMC3 cells was significantly increased when treated with Aβ (1-42) ($p < 0.001$), while further Que treatment significantly decreased LDH release ($p < 0.001$). Additionally, ML385 treatment reversed this effect, significantly increasing LDH release ($p < 0.001$). These findings suggest that Que successfully activates the NRF2/HO1 pathway and decreases cell death. Furthermore, Fig. 4B,C demonstrate that apoptosis in HMC3 cells (indicated by TUNEL-positive cells) was significantly increased by Aβ (1-42) treatment ($p < 0.001$), while further Que treatment significantly decreased apoptosis ($p < 0.001$). The reduction in apoptosis induced by Que was reversed by ML385, indicating that Que decreases cell apoptosis in Aβ (1-42)-treated microglia through activation of the NRF2/HO1 pathway. These results collectively demonstrate that Que protects microglial cells from Aβ (1-42)-induced cell death and apoptosis by activating the NRF2/HO1 pathway.

Que Alleviates Inflammation and Oxidative Stress in HMC3 Cells by Activating the NRF2/HO1 Pathway

The mRNA and protein levels of inflammatory cytokines (Fig. 5A–D) were significantly increased by Aβ (1-42) treatment ($p < 0.001$), while further Que administration significantly decreased these levels ($p < 0.001$). Additional ML385 treatment significantly increased IL-1β, IL-6, and TNF-α ($p < 0.01$). These results indicate that Que decreases Aβ (1-42)-induced inflammation in microglia only when the NRF2/HO1 pathway is not inhibited. Fig. 5E shows that Aβ (1-42)-induced increases in MDA were significantly decreased by Que treatment ($p < 0.001$), while ML385 treatment significantly increased MDA levels ($p < 0.001$). Aβ (1-42)-induced decreases in SOD and the GSH/GSSG ratio were significantly increased by Que treatment ($p < 0.001$), while ML385 treatment significantly decreased SOD and GSH/GSSG levels ($p < 0.001$) (Fig. 5F–G). These findings indicate that Que decreases oxidative stress in Aβ (1-42)-treated HMC3 cells, an effect disrupted by NRF2/HO1 pathway inhibition. These results collectively prove that Que protects Aβ (1-42)-treated HMC3 cells from inflammation and oxidative stress through activation of the NRF2/HO1 pathway.

Que Promotes Microglia M2 Polarization by Activating the NRF2/HO1

The levels of M1 phonotype-specific markers CD86 (Fig. 6A) and CD80 (Fig. 6B) were significantly increased by Aβ (1-42) treatment ($p < 0.001$), while Que treatment significantly decreased CD86 and CD80 levels ($p < 0.001$). ML385 treatment reversed this effect, significantly increasing CD86 and CD80 levels ($p < 0.01$). These findings indicate that Que decreases the Aβ (1-42)-promoted M1 microglial phenotype when the NRF2/HO1 pathway is not inhibited. Additionally, the levels of M2 phonotype-specific markers CD206 and CD163 (Fig. 6C,D) were slightly decreased by Aβ (1-42) treatment ($p < 0.01$), and Que treatment significantly increased CD206 and CD163 levels ($p < 0.01$). ML385 treatment significantly decreased CD206 and CD163 levels ($p < 0.01$), indicating that Que increases the M2 microglial phenotype when the NRF2/HO1 pathway is not inhibited. Accordingly, Que promotes microglial polarization by activating the NRF2/HO1 pathway.

Discussion

This study utilized AD model mice to prove the ameliorative effect of quercetin (Que) on Alzheimer's disease (AD), corroborating findings from previous studies [10,21, 22]. Utilizing human microglia, the mechanisms underlying the effects of Que were demonstrated to be related to the activation of the NRF2/HO1 pathway and microglia M2 polarization.

The results in this study demonstrated the significant cognition decrease in Aβ (1-42)-treated AD mice models,

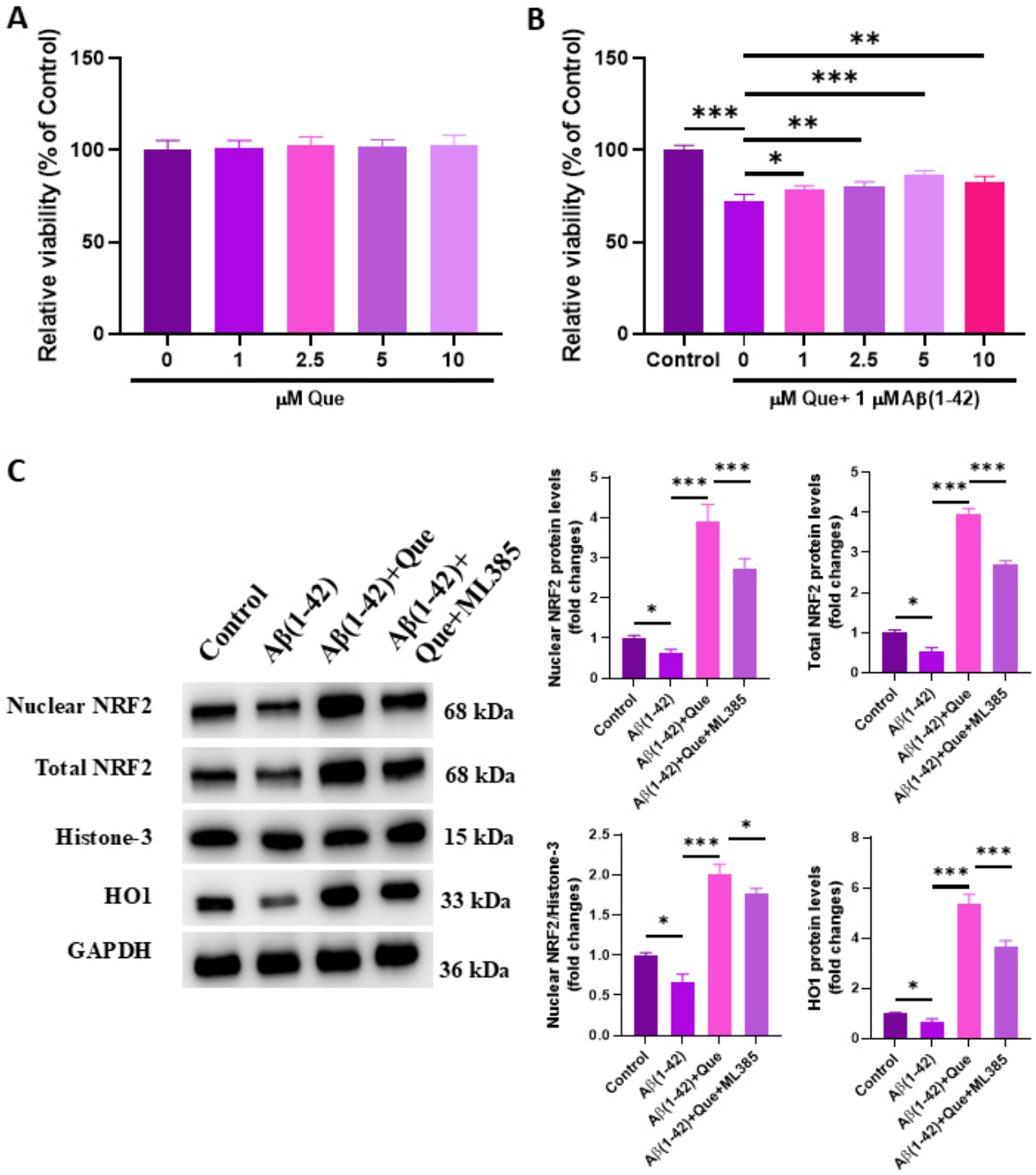

Fig. 3. Que increases cell viability and NRF2/HO1 pathway activation in microglial cells. (A,B) Cell counting kit-8 (CCK-8) assay results showing cell viability of human microglial cells HMC3 treated with different concentrations of Que (A), and with Aβ (1-42) and different concentrations of Que (B) (ANOVA). (C) Levels of NRF2/HO1 pathway-related proteins (ANOVA). n = 5. Control, HMC3 cells with no treatments; Aβ (1-42), HMC3 cells treated with Aβ (1-42) (1 μM); Aβ (1-42) + Que, HMC3 cells treated with Aβ (1-42) (1 μM) and Que (5 μM); Aβ (1-42) + Que + ML385, HMC3 cells treated with Aβ (1-42) (1 μM), Que (5 μM), and the NEF2 selective inhibitor ML385 (5 μM). *$p < 0.05$, **$p < 0.01$, ***$p < 0.001$. Abbreviations: Que, quercetin; Aβ (1-42), amyloid-beta 1-42; ML385, NRF2 inhibitor; NRF2, nuclear factor E2-related factor 2; Histone-3, Histone H3; HO1, heme oxygenase-1; GAPDH, glyceraldehyde-3-phosphate dehydrogenase.

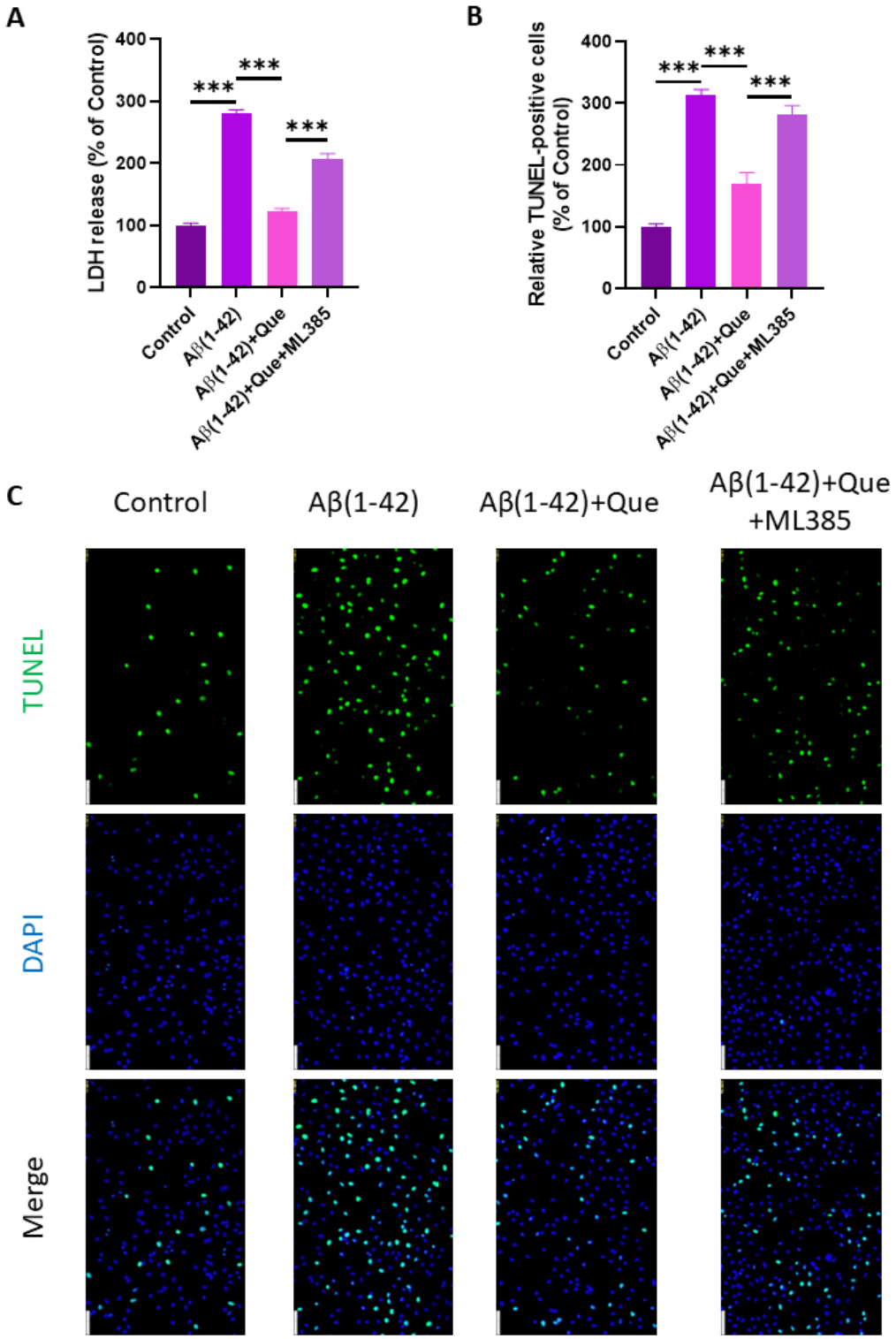

Fig. 4. Que activates the NRF2/HO1 pathway in microglial cells. (A) Lactate dehydrogenase (LDH) release levels in HMC3 cells measured by enzyme-linked immunosorbent assay (ELISA) (ANOVA). (B,C) Quantification (B) and representative images (C; scale bar: 50 µm) of apoptotic cells (ANOVA). n = 5. ***$p < 0.001$. Abbreviations: Que, quercetin; Aβ (1-42), amyloid-beta 1-42; ML385, NRF2 inhibitor; LDH, lactate dehydrogenase; TUNEL, terminal deoxynucleotidyl transferase dUTP nick-end labeling; DAPI, 4′,6-diamidino-2-phenylindole.

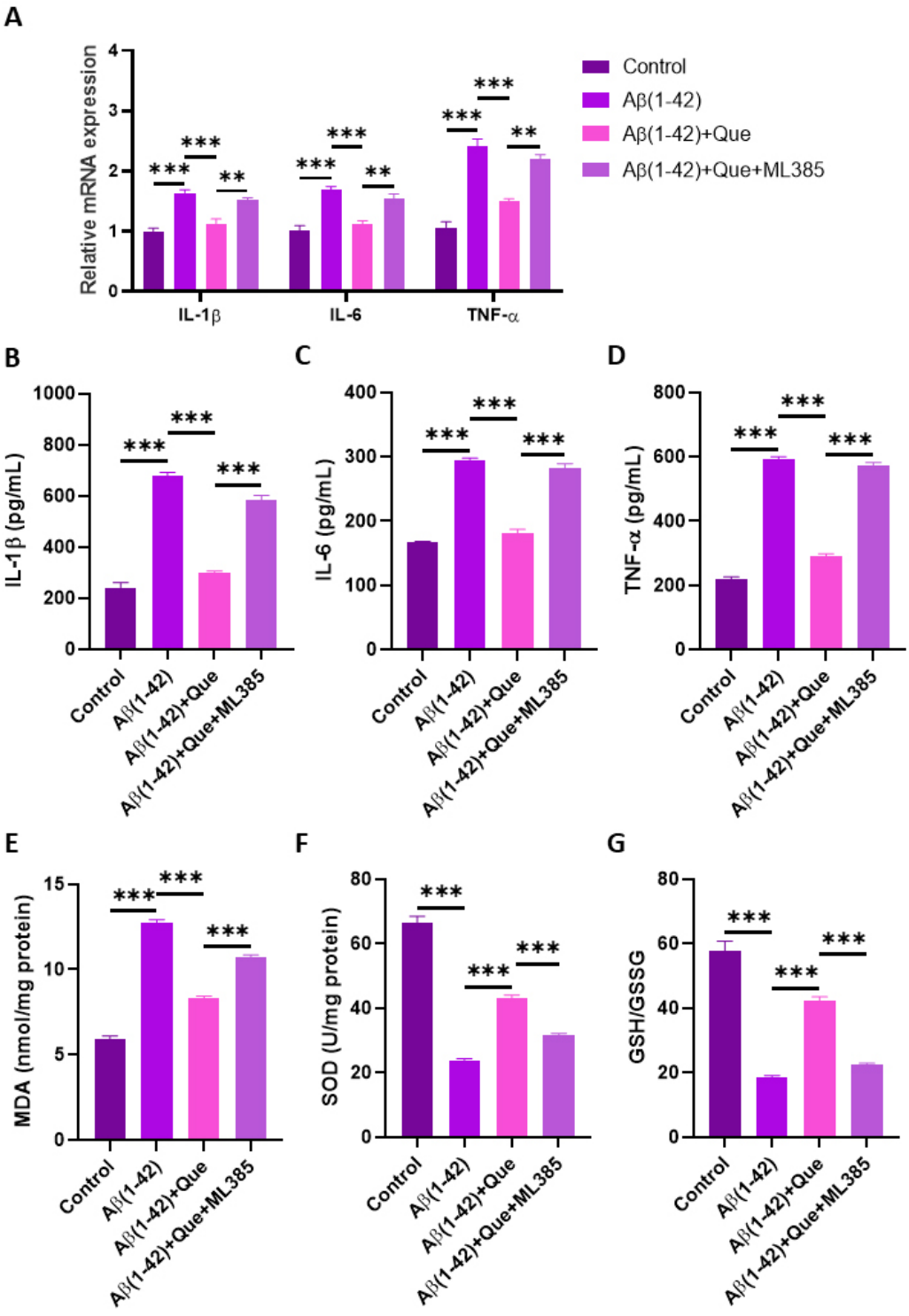

Fig. 5. Que decreases neuroinflammation and oxidative stress in HMC3 cells by activating the NRF2/HO1 pathway. (A) mRNA levels of inflammation cytokines (ANOVA). (B–D) Protein levels of inflammation cytokines detected by ELISA (ANOVA). (E–G) Protein levels of oxidative stress-related markers: malondialdehyde (MDA; E), superoxide dismutase (SOD; F), and reduced glutathione (GSH)/oxidized glutathione disulfide (GSSG; G) detected by ELISA (ANOVA). n = 5. $^{**}p < 0.01$, $^{***}p < 0.001$. Abbreviations: Aβ (1-42), amyloid-beta 1-42; Que, quercetin; ML385, NRF2 inhibitor; IL, interleukin; TNF-α, tumor necrosis factor alpha; MDA, malondialdehyde; SOD, superoxide dismutase; GSH/GSSG, glutathione/oxidized glutathione disulfide.

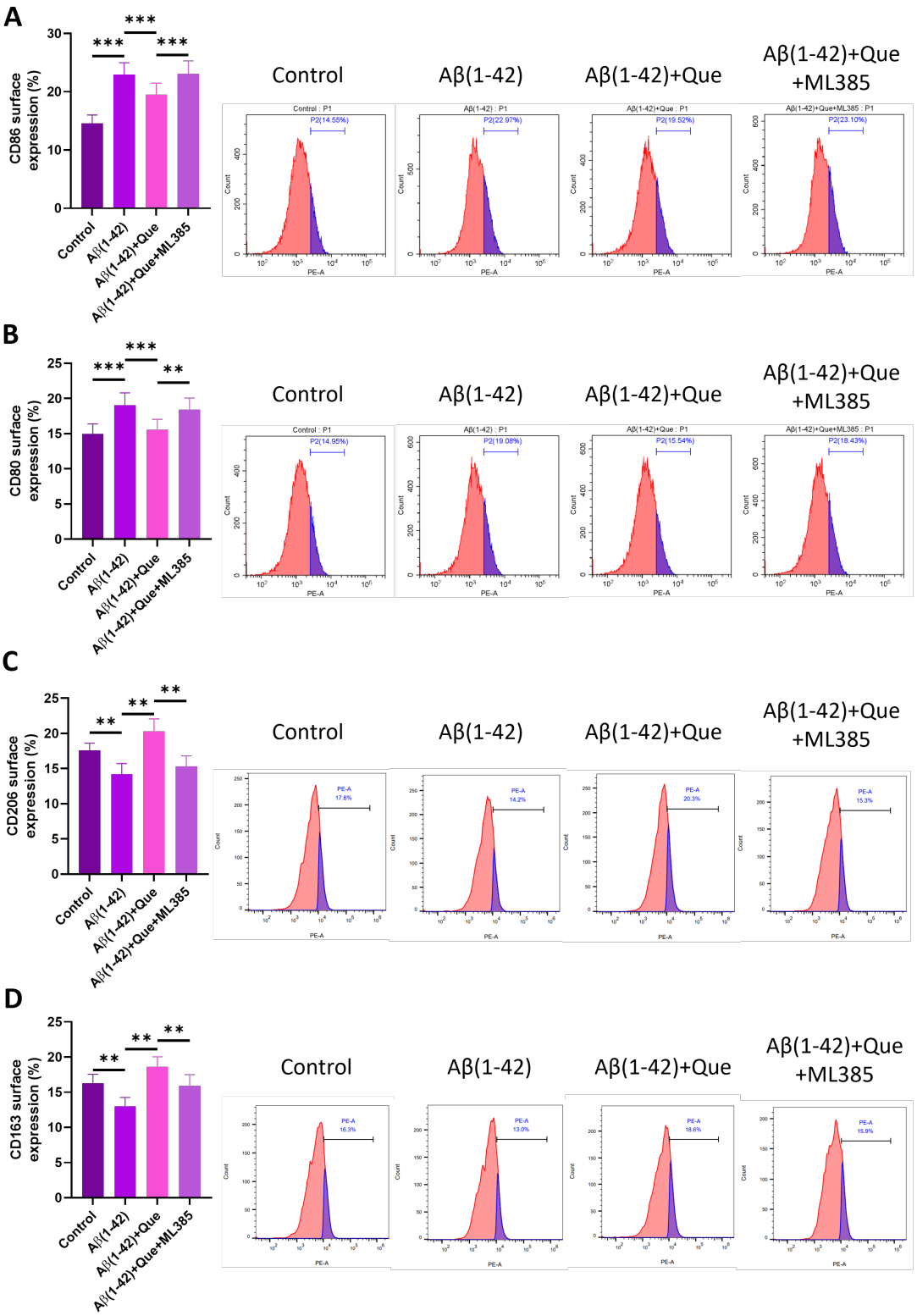

Fig. 6. Que promotes microglia M2 polarization by activating the NRF2/HO1 pathway. (A–D) Flow cytometry detection of CD86 (A), CD80 (B), CD206 (C), and CD163 (D) (ANOVA). n = 5. $^{**}p < 0.01$, $^{***}p < 0.001$. Abbreviations: Aβ (1-42), amyloid-beta 1-42; Que, quercetin; ML385, NRF2 inhibitor; CD86, cluster of differentiation 86; CD80, cluster of differentiation 80; CD206, cluster of differentiation 206; CD163, cluster of differentiation 163.

which was reversed by Que. This further proved the effectiveness of Que mitigating AD. It is well-documented that one significant event in AD is the release of proinflammatory cytokines from microglia [23]. In our study, we observed elevated levels of these cytokines in AD models, which were effectively decreased by Que, demonstrating its impact on mitigating neuroinflammation in AD. Microglia, the resident macrophages in the brain, are critical in regulating cell stress and neuroinflammation, which are closely related to neurodegenerative disorders, including AD [24,25].

In this study, we found the suppression of neuroinflammation by Que was accompanied by increased microglia polarization, characterized by a decrease in the M1 phenotype and an increase in the M2 phenotype. Since microglia polarization is a promising strategy for treating neurodegenerative disorders [26–28], the findings further validate the potential therapeutic effect of Que on such conditions. Additionally, reactive oxygen species (ROS) levels play a prominent role in the pathogenesis of AD [29]. Our study showed that Que administration reduced Aβ (1-42)-induced ROS production, confirming its effectiveness in ameliorating AD.

Multiple pathogenic processes are related to NRF2 activation and NRF2 increase, even mild and insufficient, plays a role in preventing neuronal dysfunction [30]. We observed decreased activation of the NRF2/HO1 pathway in the brains of AD mice, consistent with the previous study [20]. NRF2 and its dependent HO1 protect neurons from oxidative stress [31]. HO1 is upregulated by lethal stimuli such as oxidative stress [32], and NRF2 stabilization promotes stress response proteins, including HO1 [33]. Moreover, the role of NRF2 in attenuating AD is primarily through interference with the Aβ pathway [34]. Our study showed that Aβ (1-42) decreased NRF2/HO1 pathway activation, which was reversed by Que, highlighting its effect on NRF2 and AD.

This study combined *in vivo* (mouse model) and *in vitro* (HMC3 cell) experiments to systematically verify the effects of Que on AD, providing multifaceted evidence supporting its therapeutic potential. Cognitive abilities in mice were evaluated using the open field text, object recognition test, and Y-maze test, ensuring the reliability of the results. The research explored the role of the NRF2/HO1 signaling pathway and utilized the selective inhibitor ML385 to confirm its importance in the mechanism of action of Que. Additionally, various inflammatory cytokines, oxidative stress markers, and microglial polarization markers in brain tissue and cells were measured, providing rich data for understanding the mechanism of Que.

However, this study has several limitations. It used only a single dose and time point without assessing the effects of different doses and treatment durations. It focused primarily on short-term observations, lacking long-term effect data. The *in vitro* cell model may not fully replicate *in vivo* physiological conditions, and conclusions are based on animal models and cell experiments, which have not been validated in humans, necessitating further clinical research.

Despite these limitations, this study provides preliminary evidence for quercetin as a potential therapeutic for AD, especially its role in improving cognitive function through the NRF2/HO1 pathway, warranting further development. Future research should explore different doses and treatment durations, evaluate long-term effects and safety, and conduct clinical trials to verify its effects in AD treatment. Additionally, multicenter collaborative studies to obtain diverse population data and further explore other possible molecular mechanisms will provide a comprehensive understanding of the role of Que in AD treatment, advancing research in AD therapy.

Conclusion

Quercetin (Que) increases cell viability and, through the activation of the NRF2/HO1 pathway, decreases apoptosis, inflammation, oxidative stress, and the M1 microglial phenotype while promoting the M2 microglial phenotype in Aβ (1-42)-damaged microglia, suppressing neuroinflammation and improving cognitive function in AD mice. This study demonstrates the therapeutic potential of Que in treating AD, suggesting its potential as a viable administration for AD treatment.

Availability of Data and Materials

Data to support the findings of this study are available on reasonable request from the corresponding author.

Author Contributions

YF and XY designed the research study. JH performed the research. JH, YF and XY provided help and advice on the ELISA experiments. JH, YF and XY analyzed the data. YF and XY drafted the manuscript. All authors contributed to important editorial changes in the manuscript. All authors read and approved the final manuscript. All authors have participated sufficiently in the work and agreed to be accountable for all aspects of the work.

Ethics Approval and Consent to Participate

This study has been approved by the Ethics Committee of Shandong Second Medical University, approval No. 2024SDL065.

Acknowledgment

Not applicable.

Funding

This research was funded by Weifang Youth Talent Support Project.

Conflict of Interest

The authors declare no conflict of interest.

References

[1] Graff-Radford J, Yong KXX, Apostolova LG, Bouwman FH, Carrillo M, Dickerson BC, *et al*. New insights into atypical Alzheimer's disease in the era of biomarkers. The Lancet. Neurology. 2021; 20: 222–234.

[2] Pérez-Martínez DA. Lecanemab en la enfermedad de Alzheimer: ¿realmente estamos ante un cambio en el pronóstico de la enfermedad? [Lecanemab in Alzheimer's disease: are we really before a shift in the prognosis of the disease?]. Revista de Neurologia. 2023; 76: 185–188. (In Spanish)

[3] Scheltens P, De Strooper B, Kivipelto M, Holstege H, Chételat G, Teunissen CE, *et al*. Alzheimer's disease. Lancet (London, England). 2021; 397: 1577–1590.

[4] Can Zhang. Etiology of Alzheimer's Disease. Discovery Medicine. 2023; 35: 757–776.

[5] Singh P, Arif Y, Bajguz A, Hayat S. The role of quercetin in plants. Plant Physiology and Biochemistry: PPB. 2021; 166: 10–19.

[6] Batiha GES, Beshbishy AM, Ikram M, Mulla ZS, El-Hack MEA, Taha AE, *et al*. The Pharmacological Activity, Biochemical Properties, and Pharmacokinetics of the Major Natural Polyphenolic Flavonoid: Quercetin. Foods (Basel, Switzerland). 2020; 9: 374.

[7] Ulusoy HG, Sanlier N. A minireview of quercetin: from its metabolism to possible mechanisms of its biological activities. Critical Reviews in Food Science and Nutrition. 2020; 60: 3290–3303.

[8] Deepika, Maurya PK. Health Benefits of Quercetin in Age-Related Diseases. Molecules (Basel, Switzerland). 2022; 27: 2498.

[9] Hosseini A, Razavi BM, Banach M, Hosseinzadeh H. Quercetin and metabolic syndrome: A review. Phytotherapy Research: PTR. 2021; 35: 5352–5364.

[10] Khan H, Ullah H, Aschner M, Cheang WS, Akkol EK. Neuroprotective Effects of Quercetin in Alzheimer's Disease. Biomolecules. 2019; 10: 59.

[11] Leng F, Edison P. Neuroinflammation and microglial activation in Alzheimer disease: where do we go from here? Nature Reviews. Neurology. 2021; 17: 157–172.

[12] Yin Z, Wong S. Converging multi-modality datasets to build efficient drug repositioning pipelines against Alzheimer's disease and related dementias. Medical Review. 2022; 2: 110–113.

[13] Sanjay, Shin JH, Park M, Lee HJ. Cyanidin-3-O-Glucoside Regulates the M1/M2 Polarization of Microglia via PPARγ and Aβ42 Phagocytosis Through TREM2 in an Alzheimer's Disease Model. Molecular Neurobiology. 2022; 59: 5135–5148.

[14] Wang YH, Liu WC, Zhang JN, Geng PP, Jin XC. The role of crosstalk between cerebral immune cells and peripheral immune cells in the damage and protection of blood–brain barrier after intracerebral hemorrhage. Brain Hemorrhages. 2024; 5: 117–130.

[15] Osama A, Zhang J, Yao J, Yao X, Fang J. Nrf2: a dark horse in Alzheimer's disease treatment. Ageing Research Reviews. 2020; 64: 101206.

[16] Islamie R, Myint SLL, Rojanaratha T, Ritthidej G, Wanakhachornkrai O, Wattanathamsan O, *et al*. Neuroprotective effect of nose-to-brain delivery of Asiatic acid in solid lipid nanoparticles and its mechanisms against memory dysfunction induced by Amyloid Beta$_{1-42}$ in mice. BMC Complementary Medicine and Therapies. 2023; 23: 294.

[17] Sánchez-Rodríguez I, Gruart A, Delgado-García JM, Jiménez-Díaz L, Navarro-López JD. Role of GirK Channels in Long-Term Potentiation of Synaptic Inhibition in an In Vivo Mouse Model of Early Amyloid-β Pathology. International Journal of Molecular Sciences. 2019; 20: 1168.

[18] Lin ZH, Liu Y, Xue NJ, Zheng R, Yan YQ, Wang ZX, *et al*. Quercetin Protects against MPP$^+$/MPTP-Induced Dopaminergic Neuron Death in Parkinson's Disease by Inhibiting Ferroptosis. Oxidative Medicine and Cellular Longevity. 2022; 2022: 7769355.

[19] Lueptow LM. Novel Object Recognition Test for the Investigation of Learning and Memory in Mice. Journal of Visualized Experiments: JoVE. 2017; 55718.

[20] Yang S, Xie Z, Pei T, Zeng Y, Xiong Q, Wei H, *et al*. Salidroside attenuates neuronal ferroptosis by activating the Nrf2/HO1 signaling pathway in Aβ_{1-42}-induced Alzheimer's disease mice and glutamate-injured HT22 cells. Chinese Medicine. 2022; 17: 82.

[21] Cui Z, Zhao X, Amevor FK, Du X, Wang Y, Li D, *et al*. Therapeutic application of quercetin in aging-related diseases: SIRT1 as a potential mechanism. Frontiers in Immunology. 2022; 13: 943321.

[22] Zu G, Sun K, Li L, Zu X, Han T, Huang H. Mechanism of quercetin therapeutic targets for Alzheimer disease and type 2 diabetes mellitus. Scientific Reports. 2021; 11: 22959.

[23] Thakur S, Dhapola R, Sarma P, Medhi B, Reddy DH. Neuroinflammation in Alzheimer's Disease: Current Progress in Molecular Signaling and Therapeutics. Inflammation. 2023; 46: 1–17.

[24] Vasic V, Barth K, Schmidt MHH. Neurodegeneration and Neuro-Regeneration-Alzheimer's Disease and Stem Cell Therapy. International Journal of Molecular Sciences. 2019; 20: 4272.

[25] Kwon HS, Koh SH. Neuroinflammation in neurodegenerative disorders: the roles of microglia and astrocytes. Translational Neurodegeneration. 2020; 9: 42.

[26] Li L, Li L, Zhang J, Huang S, Liu W, Wang Z, *et al*. Disease Stage-Associated Alterations in Learning and Memory through the Electroacupuncture Modulation of the Cortical Microglial M1/M2 Polarization in Mice with Alzheimer's Disease. Neural Plasticity. 2020; 2020: 8836173.

[27] Qiu Z, Lu P, Wang K, Zhao X, Li Q, Wen J, *et al*. Dexmedetomidine Inhibits Neuroinflammation by Altering Microglial M1/M2 Polarization Through MAPK/ERK Pathway. Neurochemical Research. 2020; 45: 345–353.

[28] Jin X, Liu MY, Zhang DF, Zhong X, Du K, Qian P, *et al*. Natural products as a potential modulator of microglial polarization in neurodegenerative diseases. Pharmacological Research. 2019; 145: 104253.

[29] Ionescu-Tucker A, Cotman CW. Emerging roles of oxidative stress in brain aging and Alzheimer's disease. Neurobiology of Aging. 2021; 107: 86–95.

[30] Zhang W, Feng C, Jiang H. Novel target for treating Alzheimer's Diseases: Crosstalk between the Nrf2 pathway and autophagy. Ageing Research Reviews. 2021; 65: 101207.

[31] Deng S, Liu S, Jin P, Feng S, Tian M, Wei P, *et al*. Albumin Reduces Oxidative Stress and Neuronal Apoptosis via the ERK/Nrf2/HO-1 Pathway after Intracerebral Hemorrhage in Rats. Oxidative Medicine and Cellular Longevity. 2021; 2021: 8891373.

[32] Wang Y, Yang C, Elsheikh NAH, Li C, Yang F, Wang G, *et al*. HO-1 reduces heat stress-induced apoptosis in bovine granulosa cells by suppressing oxidative stress. Aging. 2019; 11: 5535–5547.

[33] Jyrkkänen HK, Kansanen E, Inkala M, Kivelä AM, Hurttila H, Heinonen SE, *et al*. Nrf2 regulates antioxidant gene expression evoked by oxidized phospholipids in endothelial cells and murine arteries in vivo. Circulation Research. 2008; 103: e1–9.

[34] Sharma V, Kaur A, Singh TG. Counteracting role of nuclear factor erythroid 2-related factor 2 pathway in Alzheimer's disease. Biomedicine & Pharmacotherapy = Biomedecine & Pharmacotherapie. 2020; 129: 110373.